

# A Simplified Mathematical Model for Applications of Analytical X-Ray Photogrammetry in Orthopaedics\*

Designed primarily for determination of prosthesis loosening, the expected system accuracy is on the order of 0.1 mm for distances between implanted landmark points.

## INTRODUCTION

AS PART of a cooperative research endeavor, a laboratory for the application of x-ray photogrammetry in orthopaedics has been established by the University of Washington and the Veterans Administration Hospital in Seattle. Over the past few years the analytical x-ray photogrammetric system developed to support this research has been routinely employed in such investigations as the determination of patellar tracking motions (Lippert *et al.*, 1976), and in studies of prosthesis loosening in complete hip and knee replacements (Veress and Lippert, 1978; 1979).

formulation appeared to the authors to be unnecessarily cumbersome from a practical point of view, given the nature of the fixed control frame employed for the system calibration (Veress *et al.*, 1977). For this reason an alternative mathematical model was sought. The more practical simplified (though rigorous) formulation presented in this paper is a variation of the spatial intersection model employed in stereoplotter perspective center calibration.

The spatial intersection formulation has been incorporated into the x-ray photogrammetric system and an experimental evaluation has been

---

*ABSTRACT: A simplified mathematical model for application in analytical x-ray photogrammetry is detailed, and its incorporation into an x-ray photogrammetric system primarily designed for use in orthopaedic studies of prosthesis loosening is described. Further, a computational outline of the system is given and a description of current applications in orthopaedics is presented, along with a discussion of attainable accuracy and precision.*

---

The mathematical model employed to date in the x-ray photogrammetric system (Veress *et al.*, 1977) follows the classical formulation of traditional analytical photogrammetry where all elements of interior and exterior orientation are determined. Variations on this approach have also been reported by Kratky (1975). For the present orthopaedic applications of the system, such a

carried out. However, at the time of writing (November, 1979), this updated system, which also employs a redesigned control frame, had not been used for routine patient studies. In this paper, a computational outline of the modified system is given and the mathematical formulation is developed. Further, a broad description of present applications in orthopaedics is outlined and the experimental verification of the system precision and accuracy is discussed.

## COMPUTATIONAL OUTLINE OF THE SYSTEM

The computational basis of the present analytical approach to stereo x-ray photogrammetry

\* Presented paper, Commission V, 14th Congress of the International Society for Photogrammetry, Hamburg, 13-25 July 1980.

† Presently with the Division of Surveying Engineering, The University of Calgary, Calgary, Canada T2N 1N4.

closely parallels the approach often used in traditional photogrammetric surveys: Initially, multi-line spatial intersections are carried out to determine the three-dimensional coordinates of the two anode perspective centers (analogous to spatial resection). This is then followed by two-line space intersections to compute the coordinates of the target points in the image space. To facilitate the determination of the projection center coordinates, a fixed three-dimensional control field is employed. This control frame, which is illustrated in Figures 1 and 2, provides the reference coordinate system for the image space. Further, the base of the control frame serves as a reseau plate, which allows for the correction of film deformation and certain other systematic errors inherent in the x-ray system (see Hallert, 1970, p. 20).

Figure 1 illustrates the general geometry of the x-ray photogrammetric system. In describing the role of each system component, it is helpful to consider the single ray of radiation emanating from the right anode focal spot (perspective center)  $C_R$ , passing through the plexiglass top of the frame at a point of known coordinates  $P'$ , through the reseau plate at  $P''$  and recorded on the image or film plane at  $P'''$ . This ray forms, for mathematical purposes, a straight line because the refraction effects on the beam as it passes through the plexiglass plates of the control frame are negligible (Veress *et al.*, 1977).

The initial step in the computations is the transformation of the image coordinates of point  $P'''$  on the radiograph into the coordinate system of the reseau plate, i.e., into the control frame reference system. For this transformation, a linearized form of the standard projective equation is employed. Such a transformation not only models any first order affinity within the  $x,y$  image coordinate system, but also allows for the partial compensation of second order image distortion and non-parallelism between the plane of the film

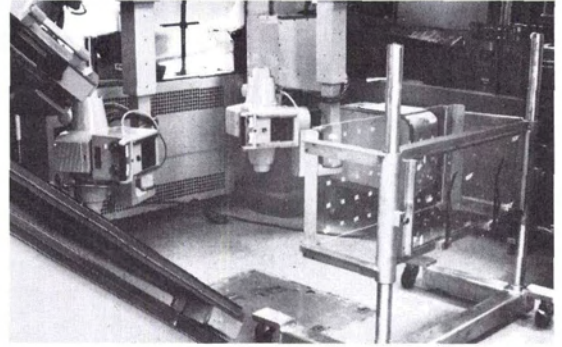


FIG. 2. X-ray control frame and anodes.

and the plane of the reseau plate. While it is desirable to have the plane of the film flush against the control frame base, there is a physical limitation in that the film must be housed in a cassette, which includes a pressure plate. The reseau crosses engraved on the control frame base have their centers filled with radio-opaque dental alloy. Such "spots" of alloy, which also mark the control points on the plexiglass top of the control frame, show clearly definable images on the x-ray photographs. A portion of a typical "resection" radiograph, showing both reseau and control frame points, is shown in Figure 3.

As a result of the initial image-to-plate coordinate transformation, the coordinates of point  $P''$  are established in the reference system of the control field. The two known points  $P''$  and  $P'$  now define the straight line along which the anode perspective center  $C_R$  lies. By determining two or more such lines passing through the control frame, the coordinates of point  $C_R$  can be obtained by spatial intersection. The mathematical model adopted for this multi-line intersection is described in the following section. A similar process is then carried out for the left anode and the determination of the coordinates of the perspective centres  $C_R$  and  $C_L$  in the reference coordinate system of the control field is thus complete.

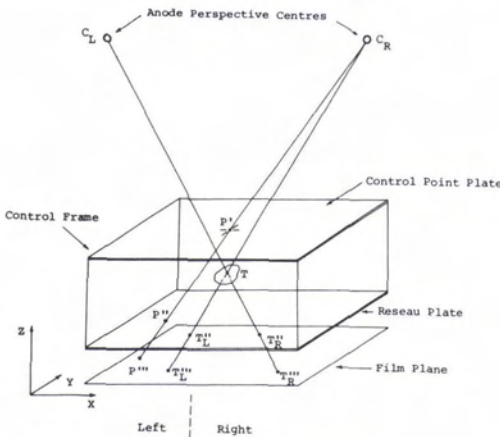


FIG. 1. System geometry.

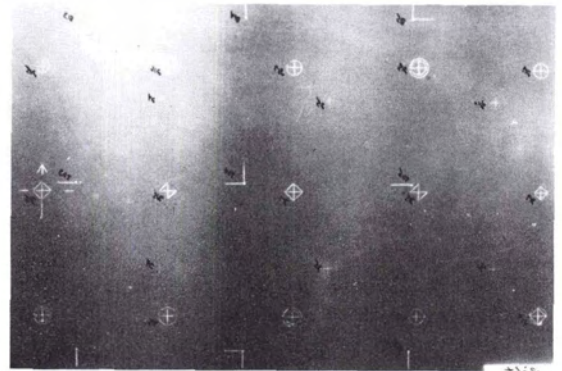


FIG. 3. Portion of "resection" radiograph.

Following the "anode resection" phase, the plexiglass top of the control frame can be removed. On subsequent replacement, this plate, on which the control points  $P'_i$  are engraved, recaptures its calibrated position to within a few tens of micrometres. With the removal of the control plate, the subject or object being imaged can be positioned in the image space between the anodes and the reseau plate, this being illustrated by the position of target  $T$  in Figure 1. The aim of the second, or intersection phase is to determine the three-dimensional coordinates of selected target points.

The two anodes are oriented in a convergent configuration and they are positioned such that a synchronized exposure will result in the right-hand side of the image plane "seeing" only radiation from the left focal spot  $C_L$  and, similarly, the left-hand side of the film area recording radiation only from the right anode  $C_R$ . As a result of the synchronised exposure, target  $T$  (see Figure 1) will be imaged in two locations,  $T_L''''$  and  $T_R''''$ , on the film plane. Following the initial transformation of image coordinates to their equivalent reseau plate coordinates, the positions of points  $T''_L$  and  $T''_R$  are obtained in the reference coordinate system. Thus, the spatial position of  $T$  is determined as being the point of intersection of the rays  $C_L T''_R$  and  $C_R T''_L$ . The algorithm used for the two-line intersection is the same as that employed for the "resection" phase of the computations.

#### MATHEMATICAL FORMULATION

A variation of the mathematical model employed in the spatial intersection method of stereoplotter perspective center calibration (see, for example, Duyet and Trinder (1976) and Ligterink (1970)) has been adopted for the present x-ray photogrammetric system application. The fundamental formula of the model is provided by the equation of a straight line joining three points in the image space: the x-ray anode perspective center  $C(x, y, z)$ , a target point  $P'(x', y', z')$ , and its corresponding image point in the plane of the reseau plate  $P''(x'', y'', z'')$ . Introducing direction cosines  $l, m$ , and  $n$ , this equation is given as

$$\frac{x - x'}{l} = \frac{y - y'}{m} = \frac{z - z'}{n} \quad (1)$$

where

$$\begin{aligned} l &= (x'' - x')/d \\ m &= (y'' - y')/d \\ n &= (z'' - z')/d \end{aligned}$$

and

$$d = \{(x'' - x')^2 + (y'' - y')^2 + (z'' - z')^2\}^{1/2}$$

Expansion of Equation 1 yields three linearly dependent equations, of which only two need be adopted:

$$\begin{bmatrix} m-l & 0 \\ n & 0-l \end{bmatrix} \begin{bmatrix} x \\ y \\ z \end{bmatrix} - \begin{bmatrix} mx' - ly' \\ nx' - lz' \end{bmatrix} = 0 \quad (2)$$

Or, in matrix notation,

$$\tilde{A}\tilde{X} - L = 0 \quad (3)$$

To obtain a point of intersection, in this case the coordinates of the focal spot  $C(x, y, z)$ , two or more lines passing through that point are required. The resulting overdetermined system can then be solved by the standard unit-weight linear least-squares technique:

$$\tilde{X} = (\tilde{A}^T \tilde{A})^{-1} \tilde{A}^T L \quad (4)$$

where  $\tilde{A}$  is the design matrix,  $L$  is the vector of absolute terms, and  $\tilde{X}$  is the vector of unknown coordinates.

Equations 2 are linear in terms of the parameters  $\tilde{X}^T = (x \ y \ z)$ ; however, they represent non-linear functions in the case where the spatial point and image point coordinates,  $(x', y', z')$  and  $(x'', y'', z'')$ , are treated as observations of known *a priori* precision. In seeking a more rigorous formulation, Equations 2 are first linearized. This gives rise to the following condition equations containing parameters  $X$ :

$$BV + AX + E = 0 \quad (5)$$

Here,  $B$  is the matrix of partial derivatives of Equations 2 with respect to the coordinates  $(x', y', z')$  and  $(x'', y'', z'')$ ,  $A$  is the matrix of partial derivatives of terms in  $\tilde{A}$  with respect to the parameters, and  $V$  and  $E$  are the residual and discrepancy vectors.

Adopting initial approximations  $x^0, y^0$ , and  $z^0$  for the parameters, the matrices  $B_i$  and  $A_i$  for a single line  $i$  are given in expanded form as

$$B_i = \begin{bmatrix} \frac{x^0 - x''}{(x'' - x')^2} & \frac{y'' - y^0}{(y'' - y')^2} & 0 & \cdots \\ \frac{x^0 - x''}{(x'' - x')^2} & 0 & \frac{z'' - z^0}{(z'' - z')^2} & \cdots \\ \cdots & \frac{x' - x^0}{(x'' - x')^2} & \frac{y^0 - y'}{(y'' - y')^2} & 0 \\ \cdots & \frac{x' - x^0}{(x'' - x')^2} & 0 & \frac{z^0 - z'}{(z'' - z')^2} \end{bmatrix}_i$$

$$A_i = \begin{bmatrix} 1/(x'' - x') & -1/(y'' - y') & 0 \\ 1/(x'' - x') & 0 & -1/(z'' - z') \end{bmatrix}_i$$

and the vectors  $V_i$  and  $E_i$  take the form

$$V_i^T = (v_x, v_y, v_z, v_{x'}, v_{y'}, v_{z'})_i$$

$$E_i = \begin{bmatrix} \frac{x^0 - x'}{x'' - x'} - \frac{y^0 - y'}{y'' - y'} \\ \frac{x^0 - x'}{x'' - x'} - \frac{z^0 - z'}{z'' - z'} \end{bmatrix}_i$$

Finally, the vector of parameters is given as  $X^T = (dx \ dy \ dz)$ , where  $dx$ ,  $dy$ , and  $dz$  are the corrections to the initial approximations  $x^0$ ,  $y^0$ , and  $z^0$ .

In solving for the unknown parameters  $X$ , normal equations are formed according to the method of least squares:

$$A^T(BW^{-1}B^T)^{-1}A X = A^T(BW^{-1}B^T)^{-1}E \quad (6)$$

where  $W$  is the weight matrix of the observations. For the present application  $W$  will be diagonal in the adjustment to determine the coordinates of each anode projection center and block diagonal for the subsequent two-ray target point intersections. The dimensions of the vectors and matrices comprising Equation 6, for a spatial intersection of  $n$  lines, are as follows:  $B(2n \times 6n)$ ,  $A(2n \times 3)$ ,  $W(6n \times 6n)$ ,  $V(6n)$ ,  $X(3)$ , and  $E(2n)$ .

The *a posteriori* precision of the parameters is given by the variance-covariance matrix

$$\sum_{xx} = \sigma_0^2 (A^T(BW^{-1}B^T)^{-1}A)^{-1} \quad (7)$$

where  $\sigma_0^2$  is the *a posteriori* variance factor.

Approximate coordinates of the point  $(x^0, y^0, z^0)$  can be calculated using the overdetermined system which is represented, albeit for a single line, by Equation 2. Computational algorithms have been formulated for the calculation of the coordinates  $(x, y, z)$  by Equation 4 and by means of the more rigorous least-squares approach, Equation 6. From a number of test computations it became apparent that the calculated coordinates  $x^0$ ,  $y^0$ , and  $z^0$  typically fell within the standard error ellipsoid around the rigorously derived estimates  $x$ ,  $y$ , and  $z$ .

In the mathematical formulation outlined, control frame target point coordinates are treated as pseudo-observed quantities subject to adjustment within the constraints imposed by their respective inverse covariance matrices. For the present experiment, the control frame was calibrated photogrammetrically. Eight exposure stations were set up, four adjacent to the reseau plate and four adjacent to the top of the control frame, which was laid on its side. The camera station configuration was such that there was a strong convergence of camera axes and an approximate photographic distance of two metres. Six reseau plate points and five control frame points were imaged along with twelve auxiliary object points which were common to all exposures. The resulting photogrammetric data were subjected to a self-calibrating bundle adjustment and the adjusted three-dimensional target point coordinates were output

with their respective *a posteriori* variances and covariances. For the adjustment, *a priori* standard errors of  $\pm 30 \mu\text{m}$  were assigned to the  $x, y$  object point coordinates ( $z = 0$ ) on the plexiglass reseau plate. These coordinates had previously been measured using the plotting table of a Wild A7. Thus, the plane of the reseau plate provided the reference coordinate system, and the points on the top plate of the control frame were then coordinated in this system.

Following the photogrammetric adjustment, a conformal transformation was performed whereby the  $x, y$  coordinates of all 45 marked control points on the plexiglass top plate (also measured using the A7) were transformed into the reference frame coordinate system using, as common points, the five points whose object space coordinates were determined photogrammetrically. Estimates of absolute coordinate precision were obtained from the *a posteriori* variance-covariance matrix.

Having described the mathematical formulation, it is useful at this point to mention a systematic perturbation of the mathematical model which the authors believe to be the main limiting factor in any enhancement of the geometric precision of the present x-ray photogrammetric system. In the spatial intersection method, as in the more traditional photogrammetric resection/intersection formulation (Veress *et al.*, 1977), each anode perspective center is assumed to be a mathematical point source of radiation. The focal spot is, however, a small surface of varying diameter, typically 0.3 to 2.0 mm. With radiation emanating at different points on the surface, a systematic disturbance of the mathematical central projection is effected. The magnitude of the resulting systematic errors in point coordinate determination can be quite significant when compared to anticipated design precision and some quantitative estimates will be given in a following section.

#### APPLICATION IN ORTHOPAEDICS

The principal area of application of the x-ray photogrammetric system described is in the determination of three-dimensional displacements between skeletal structures and prosthetic implant components. It is envisaged that the system has a wider application outside the field of orthopaedics, though the requirement for a fixed control frame for implementation of the simplified mathematical model may preclude its practical usage in some research areas—orthodontics, for example. In the following paragraphs a brief outline of the procedure adopted in applying the x-ray photogrammetric system to the determination of prosthesis loosening in complete hip and knee replacements is given.

Under the present hypothesis (Veress and Lipfert, 1979), a prosthesis is deemed to be loose when about 1 mm of interface motion exists be-

tween the implant and the socket in the bone. In order to measure prosthesis/bone interface motion, stainless steel balls are implanted in both the prosthesis and the lateral cortex of the bone to serve as landmarks. By taking two simultaneous radiographs of the patient in an unloaded position, that is, where no body weight is exerted on the prosthesis, three-dimensional coordinates of the landmarks can be determined. Following the x-rays of the non-weight bearing position, a similar pair of radiographs (or one large single image) is obtained with the patient exerting his body weight on the leg being examined. The three-dimensional coordinates of the landmarks in this loaded or weight bearing position are then computed and after an appropriate transformation, or calculation of point-to-point distances, the extent of relative prosthesis motion can be evaluated.

In applying the x-ray photogrammetric system in orthopaedic studies of prosthesis loosening, the individual steps are as follows: Initially, the control frame and the anodes are set up in the desired geometric configuration (anode separation approximately 1.1 m, a convergence angle subtended by the projection axes of  $40^\circ$  and a photographic distance of about 1.7 m). A pair of radiographs is then taken to provide data for the "resection" phase. Following this, the top plate of the control frame is removed, leaving only the reseau plate, and the patient is positioned in the image space. Radiographs are then taken for the unloaded and loaded positions and, if desired, the procedure for the "resection" phase may then be repeated to ensure that there was no movement between the anodes and the control frame during the process. In the foregoing, only a broad outline of the application to prosthesis loosening determination has been given. For a more detailed discussion the reader is referred to Veress and Lippert (1978), where a description of the system prior to its modification is also given.

#### DISCUSSION OF SYSTEM PRECISION AND ACCURACY

In determining the extent of prosthetic component loosening, data obtained from the x-ray photogrammetric survey of the implant in the bone, for both the weight and non-weight bearing positions, are compared. At present there are two approaches to this determination. First, if only the magnitude of the relative displacement between the prosthesis and the landmark system in the bone is required, this can be achieved by examining the point-to-point distance variations encountered between the loaded and unloaded positions. Second, if rotational components of any motion are sought, a three-dimensional conformal transformation is carried out, mapping coordinates obtained in the weight bearing position into their equivalent non-weight bearing position coordinate values. The landmark system in the cortex of

the bone provides the common points for this transformation. The following discussion will be confined to an assessment of the accuracy of the x-ray photogrammetric system as indicated by the *a posteriori* precision and accuracy of distances and distance discrepancies obtained in experimental test applications.

As a result of the x-ray photogrammetric survey, two or more sets of landmark coordinates are obtained along with estimates of the precision of these three-dimensional coordinate values. The variance-covariance matrix  $\Sigma_{T_i}$  of the coordinates of a particular target point  $T_i$  provides a measure of its absolute precision within the reference coordinate system. However, since loosening is determined through an examination of distance variations, it is appropriate to consider the reliability of the calculated distances. Applying the general law of propagation of variances, the variance of the distance  $d_{ij}$  between points  $T_i$  and  $T_j$  is given by

$$\sigma_{d_{ij}}^2 = \mathbf{C}_{ij} \Sigma \mathbf{C}_{ij}^T \quad (8)$$

where

$$\mathbf{C}_{ij} = \begin{bmatrix} -l & -m & -n & l & m & n \end{bmatrix}_{ij}$$

$$\Sigma = \begin{bmatrix} \Sigma_{T_i} & 0 \\ 0 & \Sigma_{T_j} \end{bmatrix}$$

$$\Sigma_{T_i} = \begin{bmatrix} \sigma_x^2 & \sigma_{xy} & \sigma_{xz} \\ \text{symm.} & \sigma_y^2 & \sigma_{yz} \\ & & \sigma_z^2 \end{bmatrix} T_i$$

$l, m, n$  = direction cosines, see Equation 1.

The structure of  $\Sigma$  becomes block-diagonal because the coordinates of the points  $T_i$  and  $T_j$  are computed by independent two-line intersections.

Appropriate statistical tests can be applied to ascertain whether the distance difference in question represents significant prosthesis loosening. As has been mentioned, a pain and discomfort threshold motion value is thought to be about 1 mm. Using the present x-ray photogrammetric system, with the geometric configuration described, a typical magnitude range for the distance standard error is  $45 \mu\text{m} < \sigma_{d_{ij}} < 60 \mu\text{m}$ . Thus, significant motion can be determined at well below the 1-mm level, since the standard error of a distance difference  $\sigma_{\Delta d_{ij}}$  has an upper bound value of about  $\pm 80 \mu\text{m}$ .

The value of the standard error  $\sigma_{d_{ij}}$  indicated by Equation 8 is determined on the assumption that each anode perspective center is a mathematical point. To quantitatively assess the effects on final distance determinations due to perturbations caused by rays emanating over the surface of the focal spot, a number of experimental determinations were made of known fixed distances, both on a simulated subject model and on the control frame. Comparisons with known photogrammetrically determined distances were made, and these

indicated that a more practical estimate of  $\sigma_{d_{ij}}$  would be about  $\pm 90 \mu\text{m}$  when using a digitizer of about  $40 \mu\text{m}$  accuracy for the initial image coordinate observations. For example, in one test of 105 distances, the discrepancies ranged in magnitude from  $1 \mu\text{m}$  to  $230 \mu\text{m}$ , with an overall measure of accuracy being the RMS value of  $\pm 97 \mu\text{m}$ . Adopting the value  $\sigma_{d_{ij}} = \pm 90 \mu\text{m}$  yields a distance difference precision estimate of  $\sigma_{\Delta d_{ij}} = \pm 130 \mu\text{m}$ . However, in a more recent test, employing a digitizing table of somewhat higher accuracy to that used in the above mentioned application, a value  $\sigma_{d_{ij}} = \pm 65 \mu\text{m}$  was obtained from a sample of 36 distances.

In summary, for the present geometric configuration, which is designed primarily for orthopaedic application in the determination of prosthesis loosening, the expected accuracy of the x-ray photogrammetric system described is on the order of 0.1 mm for distances between implanted landmark points. While the *a posteriori* precision of landmark  $x$  and  $y$  coordinates is of a slightly higher order, it is considered that the main factor limiting attainable precision and accuracy, apart from the resolution of the digitizer presently employed for the initial  $x, y$  image coordinate measurements (about  $\pm 40 \mu\text{m}$ ), is the perturbation to the rigid central projection model. And, as a secondary factor, components of residual systematic error introduced in the photogrammetric calibration of the control frame.

#### ACKNOWLEDGMENTS

This work has been partially supported by the United States Veterans Administration under

Grant V663P-1006. The useful discussions held with the co-principal investigators, Dr. F. G. Lippert III and Dr. S. A. Veress, are gratefully acknowledged.

#### REFERENCES

- Duyet, T. L., and J. C. Trinder, 1976. *Stereoplotter Perspective Centre Calibration*, Unisurv G24, Univ. of N.S.W., Sydney, 81-100.
- Hallert, B., *X-Ray Photogrammetry, Basic Geometry and Quality*, Elsevier, Amsterdam, 154.
- Kratky, V., 1975. Analytical X-Ray Photogrammetry in Scoliosis, *Proceedings of the Symposium on Close-Range Photogrammetry*, Urbana.
- Ligterink, G. H., 1970. Aerial Triangulation by Independent Models—the Coordinates of the Perspective Centre and their Accuracy, *Photogrammetria*, Vol. 26, No. 1.
- Lippert, F. G., T. Takamoto, and S. A. Veress, 1976. Determination of Patellar Tracking Patterns by X-Ray Photogrammetry, *Proceedings of ASP Fall Meeting*, Seattle, pp. 107-121.
- Veress, S. A., and F. G. Lippert, 1978. A Laboratory and Practical Application of X-Ray Photogrammetry, *Proceedings of ASP 44th Annual Meeting*, Wash., D.C., pp. 409-421.
- , 1979. Using X-Ray Photogrammetry in Orthopaedics to Determine Prosthesis Loosening, *Photogrammetric Engineering and Remote Sensing* (in press).
- Veress, S. A., F. G. Lippert, and T. Takamoto, 1977. An Analytical Approach to X-Ray Photogrammetry, *Photogrammetric Engineering and Remote Sensing*, Vol. 43, No. 12.

(Received 19 January 1980; revised and accepted 9 November 1980)

### Forthcoming Articles

- G. Ross Cochrane and G. H. Browne, Geomorphic Mapping from Landsat-3 Return Beam Vidicon (RBV) Imagery.
- Edgar L. Ferguson, Dennis G. Jorde, and John J. Sease, Use of 35-mm Color Aerial Photography to Acquire Mallard Sex Ratio Data.
- Robert B. Forrest, Simulation of Orbital Image-Sensor Geometry.
- Joachim K. Höhle and Alfred Jakob, New Instrumentation for Direct Photogrammetric Mapping.
- T. J. Jackson, A. Chang, and T. J. Schmutge, Aircraft Active Microwave Measurements for Estimating Soil Moisture.
- L. Daniel Maxim, Leigh Harrington, and Mary Kennedy, A Capture-Recapture Approach for Estimation of Detection Probabilities in Aerial Surveys.
- L. Daniel Maxim, Harrison D. Weed, Leigh Harrington, and Mary Kennedy, Intensity Versus Extent of Coverage.
- L. Daniel Maxim, Leigh Harrington, and Mary Kennedy, Alternative "Scale Up" Estimators for Aerial Surveys where both Detection and Classification Errors Exist.
- E. J. Milton, Does the Use of Two Radiometers Correct for Irradiance Changes During Measurements?
- E. Karl Sauer, Hydrogeology of Glacial Deposits from Aerial Photographs.
- Nobuo Sawada, Masatsugu Kidode, Hidenori Shinoda, Haruo Asada, Masayuki Iwanaga, Sadakazu Watanabe, Ken-Ichi Mori, and Minoru Akiyama, An Analytic Correction Method for Satellite MSS Geometric Distortions.
- F. L. Scarpace, B. K. Quirk, R. W. Kiefer, and S. L. Wynn, Wetland Mapping from Digitized Aerial Photography.
- R. Welch and Wayne Marko, Cartographic Potential of a Spacecraft Line-Array Camera System: Stereosat.
- R. Welch, P. N. Slater, H. Tiziani, and J. C. Trinder, ISP Image Quality Working Group Activities, 1976-1980.
- Kam W. Wong and Alan P. Vonderohe, Planar Displacement by Motion Parallax.